

Synthesis of Few-walled Boron Nitride Nanotubes using Triple DC Thermal Plasma Jet System with Hydrogen Injection

M. Kim¹, J. H. Oh¹, B. I. Min¹, Y. H. Lee¹, S. H. Hong¹, T. H. Kim² and S. Choi^{1,2,*}

¹Department of Nuclear and Energy Engineering, Jeju National University, Jeju 63243, Republic of Korea

²Institute for Nuclear Science and Technology, Jeju National University, Jeju 63243, Republic of Korea

Abstract: Few-walled boron nitride nanotubes were synthesized in the triple DC thermal plasma jet system with hydrogen injection. The role of hydrogen was investigated with thermodynamic equilibrium reaction calculations. The calculation revealed that injection of hydrogen in the reactor prominently prohibits the liberated N from rapidly recombining to N₂, instead forming NH, NH₂, and N₂H₂ gas, which leads formation of B-N-H intermediates that eventually grow to BNNT through dehydrogenation and early nucleation of boron. As an experimental result, it was achieved to synthesize few-walled (≤ 3 walls), small-diameter (< 5 nm), and high-crystalline BNNT by virtue of hydrogen as a reactant gas.

Keywords: Triple DC thermal plasma jet, Synthesis, Boron nitride nanotubes, Hydrogen

1. Introduction

Boron Nitride Nanotubes (BNNT) have triggered considerable attention from industrial fields due to their tantalizing characteristics such as mechanical [1,2], electron field emission [3], piezoelectric [4], thermal [5,6], optical [7,8], purification [9], biocompatible [10] properties since it synthesized in 1995 [10]. In spite of this considerable attention, the low production rate is a conclusive obstacle to apply them in the various industrial fields. Therefore, it requires to improve the BNNT synthesis system to a broad possibility of them into industrial applications such as optoelectronic device and reinforcements for structural composites.

Various methods have demonstrated to synthesize BNNT since the first synthesis using plasma discharge; laser ablation/vaporization [11], the arc discharge [12,13], chemical vapour deposition [14], and ball milling and annealing [15,16]. From these works, the feasibility of BNNT synthesis was examined in a laboratory-scale but still remains tough in a pilot-scale, resulting in the quantity and quality of the produced BNNT are far from those of carbon nanotubes. In the view of scalable synthesis of BNNT, Smith et al. initially showed production of 60 mg of extraordinarily long, highly crystalline BNNT without catalyst during 30 minutes using laser ablation [17]. Huang et al. also demonstrated production of ~50 mg of BNNT which have average diameters of below 10 nm and lengths of up to tens of μm for 3 hours using chemical vapour deposition [18]. These results lead highly progress in the production technique of BNNT but a noteworthy advance in industrially scalable production of BNNT is recently achieved using induction thermal plasma process which reached the continuous production of highly crystalline, small-diameter of BNNT at a rate approaching 20 g/h with help of hydrogen [19].

In this work, we suggest that it is suitable for a scalable synthesis of BNNT to introduce triple direct current thermal plasma jet system with extensively merged high

temperature region as well as easily injection of precursor into the plasma flame [20]. Additionally, it has more advantage to produce small-diameter BNNT since DC thermal plasma jet provides higher quenching rate than induction thermal plasma jet in general. The effect of hydrogen in the BNNT synthesis process is thermodynamically discussed with intermediate phases.

2. Experimental detail

2.1 Calculation of thermodynamic equilibrium reaction

The synthesis process for BNNT from the considerably high temperature to quenching temperature areas was analysed. The thermodynamic equilibrium equations were calculated with commercial software of HSC Chemistry (Ver. 9.1.1, Outotec Research Oy, Finland). Whether it is a spontaneous chemical reaction can be figured out with the Gibbs free energy which can be derived from enthalpy and entropy in the given temperature range [21]. The reaction calculations for various nitro-hydrogen and borane gas were conducted to demonstrate routes from them to B-N-H intermediates which are known to be grown as BNNT [19]. In order to prove the fact that H₂ gas is important factor to synthesize BNNT, the various formation reaction from NH and BH gas were calculated with H₂ gas. Subsequently, boron nitride hydrogen (BNH) and polyiminoborane (BNH₂) formation reaction were calculated with the formed NH with BH gas. In the chemical reaction, temperature range was given from 500 K to 12,000 K, and pressure was fixed at atmospheric pressure.

2.2 Synthesis of boron nitride nanotubes

The schematic diagram of triple DC thermal plasma jet system for the synthesis of BNNT is shown in Fig. 1. The system consists of three thermal plasma torches (Plasnix Co., Ltd., Republic of Korea), vertical and horizontal axis reactors (R-1~R-7), three power supplies, cyclone filter,

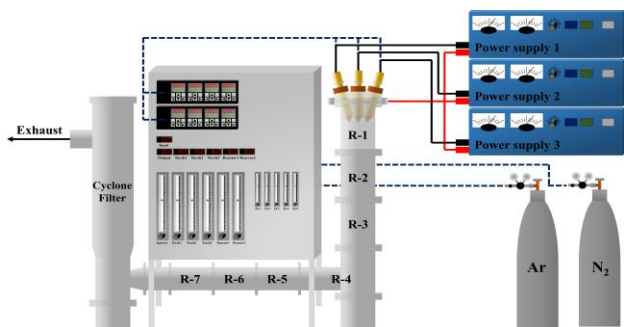


Fig. 1. The illustration of triple DC thermal plasma jet system for the synthesis of boron nitride nanotubes.

Table I. Experimental condition for the synthesis of boron nitride nanotubes.

Total power (kW)	21.4
Chamber pressure (kPa)	101.325
Plasma forming gas (slpm)	4 (Ar), 8 (N ₂)
Carrier gas (slpm)	5 (Ar)
Reactant gas (slpm)	8 (H ₂)

and a control box of cooling waters and gases. The experimental conditions are summarized in Table I. hexagonal boron nitride (h-BN) powder (~1 μm, 98%, 255475, Sigma-Aldrich, Inc., USA) was used as a precursor. The individual thermal plasma jet was generated by 4 L/min of Ar and 8 L/min of N₂ mixed gases under atmospheric pressure, and 8 L/min of H₂ as reactant gas was injected from upper part of R-1. The input power of each torch was about 6.9~7.5 kW at fixed current of 100 A. The precursor with 5 L/min of Ar carrier gas was injected into the coalesced plasma flame from the top of the triple torches, and feeding rate was about 0.5~0.6 g/min.

3. Results and discussion

3.1 Thermodynamic equilibrium calculation

The nitrogen is essential source for BNNT growth, decomposing in very high temperature (>7,000 K) and quickly recombining into N₂ at also high temperature (<7,000 K) regions. The direct reaction of B and N₂ into a h-BN phase also hardly occur attributable to the strong triple bond of nitrogen. However, hydrogen prevent to recombine nitrogen diatomic molecules as forming various NH and BH radical and gas in the high temperature regions which is provided by merged plasma flame.

Fig. 2(a) shows H₂ (reactant) and N₂ (plasma forming gas) decomposed into H and N radical ion (>10,000 K), which leads NH, NH₂, and N₂H₂ gas and NH radical ion formation (<9,500 K), and Fig. 2(b) also reveals BN (Precursor) and H₂ (Reactant) gas combine into N₂H₂ gas (>7,000 K). In the reaction with BN and H₂ gas, it hardly occurs to form NH and NH₂ gas in the all temperature areas. From these results, it was estimated that the presence of hydrogen highly prevents the decomposed N to rapidly combine to produce N₂, instead forming NH, NH₂, and N₂H₂ gas.

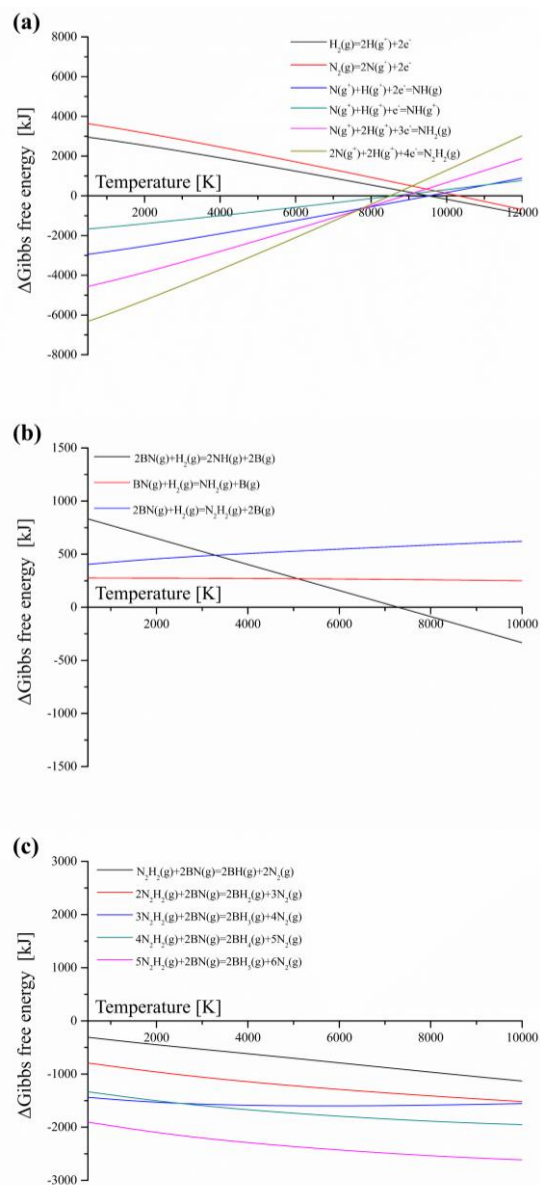


Fig. 2. The change of Gibbs free energy by thermodynamic equilibrium calculation for (a) H and N radical ion formation reactions, (b) NH, NH₂, and N₂H₂ gas formation reactions, and (c) various borane formation reaction.

Especially, Fig. 2 (c) shows NH₂ and N₂H₂ gas dominantly react with the BN gas in all temperature regions. It revealed that these gas are key source to form borane gas which is essential source of B-N-H intermediates. In addition, it was figured out that BN gas also conducts important role in formation borane gas, meaning that injecting h-BN as precursor is more desirable to synthesize BNNT than amorphous boron. Eventually, these B-N-H intermediates grows to BNNT through dehydrogenation reaction as well as early nucleation of boron nuclei [19].

As a result, NH radical ion, NH₂, and N₂H₂ gas formation reaction in the high temperature regions is largely available through hydrogen-rich atmosphere, which is crucial factor of scalable BNNT growth in the system.

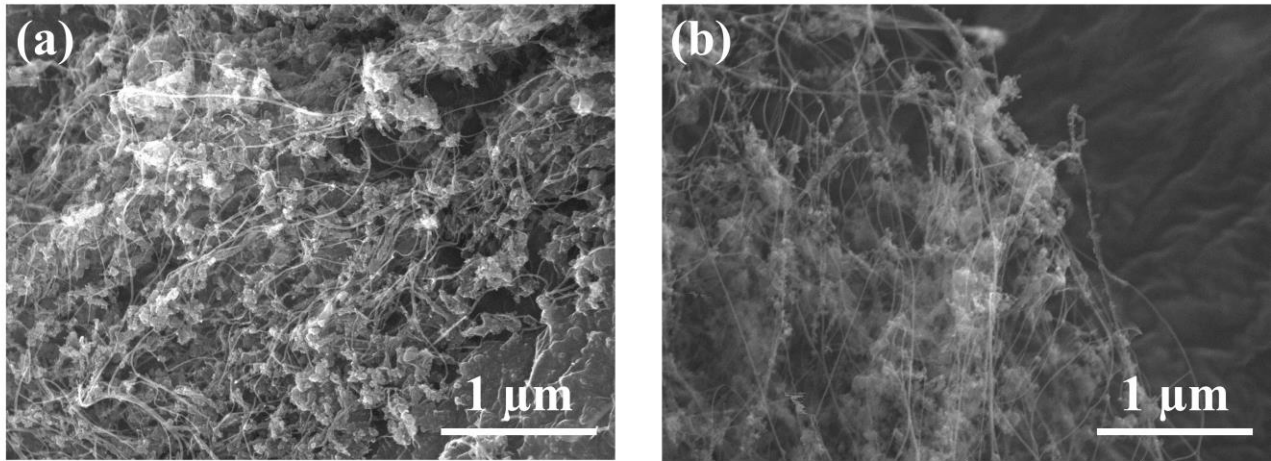


Fig. 3. The morphological property of the grown BNNT. FE-SEM images of the BNNT from (a) the vertical reactor and (b) the horizontal reactor.

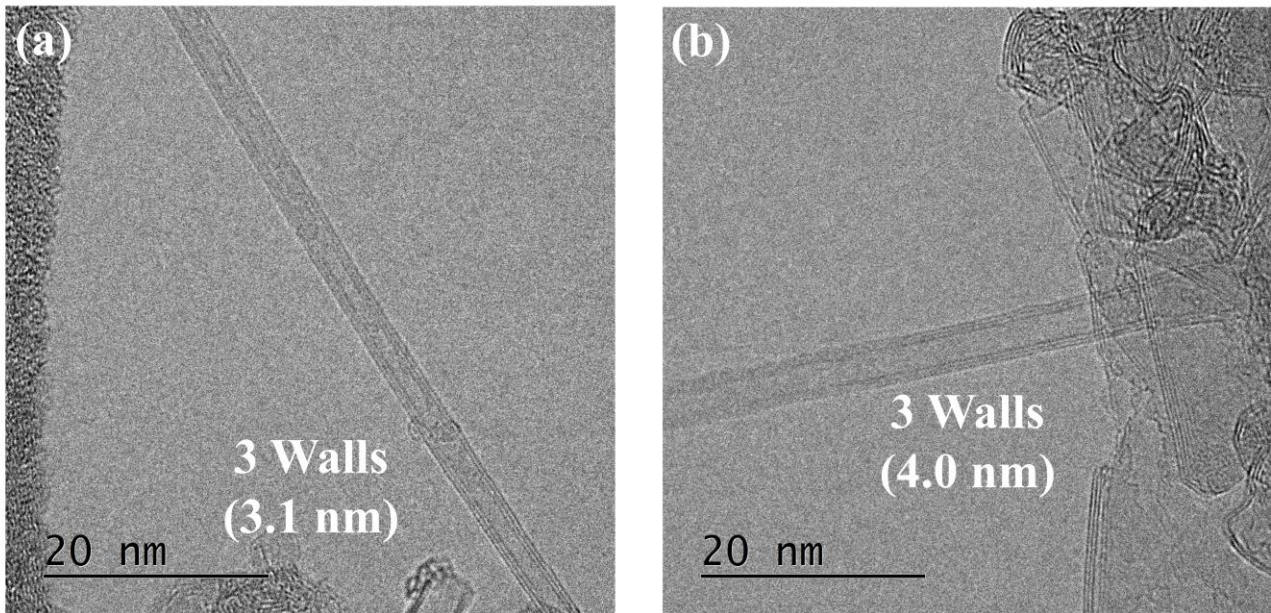


Fig. 4. The few walled and small diameter structure of the synthesized BNNT from the HR-TEM. (a) A three-walled BNNT whose diameter is about 3.1 nm, and collected from the vertical axis. (b) A three-walled BNNT whose diameter is about 4.0 nm, and collected from the horizontal axis.

3.2 Synthesis of few-walled boron nitride nanotubes

Fig. 3(a) and (b) each shows FE-SEM image of BNNT collected from the vertical and horizontal reactors. The fabric material such as tangled threads successfully formed in the triple DC thermal plasma jet system. It is also observed that some particles attached on the fabric material, but elimination of such impurities is possible through purification processes such as chemical reaching, polymer wrapping, and solution extraction. In addition, it is also observed that length of fabric material from horizontal reactor is much longer than that of vertical reactor as shown in Fig. 3(a) and (b), which suggests residence time of precursor in the reactor have influence on length of grown

BNNT. The vertical reactors are more close to the plasma flame, meaning that the grown BNNT in these reactors have shorter time to grow as BNNT than horizontal reactors. TEM analysis validated that the fabric material from the vertical and horizontal reactors has tubular structures which are straight and parallel to the axis of the tube as shown in Fig. 4. The most common number of walls was between 2 and 3; the majority of the BNNT are three-walled. These tubular structures have diameters below 5 nm. In addition, the multi-walled BNNT had highly crystalline structure without drawbacks like bamboo structure which are derived from relatively low temperature synthesis. These highly crystalline structure

was stemmed from the thermal plasma synthesis process which provides enough time for B-N-H intermediates to immediately form crystal structure in the high temperature regions.

3. Conclusion

Thermodynamic equilibrium reaction calculation and synthesis experiments were mutually conducted in order to produce few-walled (≤ 3 walls), small-diameter (< 5 nm) BNNT. These thermodynamical reaction calculation demonstrated that the injection of hydrogen as reactant gas in the plasma flame which heats up to 12,000 K remarkably prevents the decomposed N to quickly recombine into N_2 on behalf of forming NH, NH_2 , N_2H_2 gas. These gases generate various borane gas, which leads formation of B-N-H intermediates which eventually grow to BNNT through dehydrogenation reaction with early nucleation of boron in the quenching process. The triple DC thermal plasma jet system which is divided into 7 regions provides extensively coalesced high temperature areas as well as configuration advantage of easily penetration of precursor into the plasma flame. From these divided areas, it was founded out that residence time of precursor has influence on crystallinity and length of grown BNNT; length and crystallinity of the BNNT increased as being far from the plasma flame.

4. References

- [1] N.G. Chopra, A. Zettl, Solid State Communications, **105**, 297–300 (1998).
- [2] D. Goldberg, X.D. Bai, M. Mitome, C.C. Tang, C.Y. Zhi, Y. Bando, Acta Materialia, **55**, 1293-1298 (2007).
- [3] V. Meunier, C. Roland, J. Bernholc, M.B. Nardelli, Applied Physics Letters, **81**, 46-48 (2002).
- [4] E.J. Mele, P. Král, Physical Review Letters, **88**, 568031-568034 (2002).
- [5] Y. Chen, J. Zou, S.J. Campbell, G. L. Caer, Applied Physics Letters, **84**, 2430-2432 (2004).
- [6] C.W. Chang, A.M. Fennimore, A. Afanasiev, D. Okawa, T. Ikuno, H. Garcia, D. Li, A. Majumdar, A. Zettl, Physical Review Letters, **97**, 1-4 (2006).
- [7] J.S. Lauret, R. Arenal, F. Ducastelle, A. Loiseau, M. Cau, B. Attal-Tretout, E. Rosencher, L. Goux-Capes, Physical Review Letters, **94**, 1-4 (2005).
- [8] R. Arenal, O. Stéphan, M. Kociak, D. Taverna, A. Loiseau, C. Colliex, Physical Review Letters, **95**, 1-4 (2005).
- [9] T.A. Hilder, D. Gordon, S.H. Chung, Small, **5**, 2183-2190 (2009).
- [10] N.G. Chopra, R.J. Luyken, K. Cherrey, V.H. Crespi, M.L. Cohen, S.G. Louie, A. Zettl, Science, **269**, 966-967 (1995).
- [11] D. Golberg, Y. Bando, M. Eremets, K. Takemura, K. Kurashima, H. Yusa, Applied Physics Letters, **69**, 2045-2047 (2002).
- [12] A. Loiseau, F. Willaime, N. Demoncy, G. Hug, H. Pascard, Physical Review Letters, **76**, 4737-4730 (1996).
- [13] Y. Shimizu, Y. Moriyoshi, H. Tanaka, S. Komatsu, Applied Physics Letters, **75**, 989-931 (1999).
- [14] C.H. Lee, J. Wang, V.K. Kayatsha, J.Y. Huang, Y.K. Yap, Nanotechnology, **19** (2008).
- [15] Y. Chen, L.T. Chadderton, J.F. Gerald, J.S. Williams, Applied Physics Letters, **74**, 2960-2962 (1999).
- [16] J. Yu, Y. Chen, R. Wuhrer, Z. Liu, S.P. Ringer, Chemistry of Materials, **17**, 5172-5176 (2005).
- [17] M.W. Smith, K.C. Jordan, C. Park, J. Kim, P.T. Lillehei, R. Crooks, J.S. Harrison, Nanotechnology, **20**, 505604 (2009).
- [18] Y. Huang, J. Lin, C. Tang, Y. Bando, C. Zhi, T. Zhai, B. Dierre, T. Sekiguchi, D. Golberg, Nanotechnology, **22**, 145602 (2011).
- [19] K.S. Kim, C.T. Kingston, A. Hrdina, M.B. Jakubinek, J. Guan, M. Plunkett, B. Simard, ACS Nano, **8**, 6211-6220 (2014).
- [20] K. Ramachandran, H. Nishiyama, Journal of Physics D: Applied Physics, **36**, 1198-1203 (2003).
- [21] H.B. Levine, Journal of Chemical Physics, **36**, 1957-1959 (1994).